Land water storage variability over West Africa estimated by Gravity Recovery and Climate Experiment (GRACE) and land surface models

M. Grippa,[1] L. Kergoat,[1] F. Frappart,[1] Q. Araud,[1] A. Boone,[2] P. de Rosnay,[3] J.-M. Lemoine,[4] S. Gascoin,[5] G. Balsamo,[3] C. Ottlé,[6] B. Decharme,[2] S. Saux-Picart,[7] and G. Ramillien[1]

Received 2 November 2009; revised 31 January 2011; accepted 10 February 2011; published 28 May 2011.

[1] Land water storage plays a fundamental role in the West African water cycle and has an important impact on climate and on the natural resources of this region. However, measurements of land water storage are scarce at regional and global scales and especially in poorly instrumented endorheic regions, such as most of the Sahel, where little useful information can be derived from river flow measurements and basin water budgets. The Gravity Recovery and Climate Experiment (GRACE) satellite mission provides an accurate measurement of the terrestrial gravity field variations from which land water storage variations can be derived. However, their retrieval is not straightforward, and different methods are employed, which results in different water storage GRACE products. On the other hand, water storage can be estimated by land surface modeling forced with observed or satellite-based boundary conditions, but such estimates can be highly model dependent. In this study, land water storage by six GRACE products and soil moisture estimations by nine land surface models (run within the framework of the African Monsoon Multidisciplinary Analysis Land Surface Intercomparison Project (ALMIP)) are evaluated over West Africa, with a particular focus on the Sahelian area. The water storage spatial distribution, including zonal transects, its seasonal cycle, and its and interannual variability, are analyzed for the years 2003–2007. Despite the nonnegligible differences among the various GRACE products and among the different models, a generally good agreement between satellite and model estimates is found over the West Africa study region. In particular, GRACE data are shown to reproduce well the water storage interannual variability over the Sahel for the 5 year study period. The comparison between satellite estimates and ALMIP results leads to the identification of processes needing improvement in the land surface models. In particular, our results point out the importance of correctly simulating slow water reservoirs as well as evapotranspiration during the dry season for accurate soil moisture modeling over West Africa.

Citation: Grippa, M., et al. (2011), Land water storage variability over West Africa estimated by Gravity Recovery and Climate Experiment (GRACE) and land surface models, *Water Resour. Res.*, *47*, W05549, doi:10.1029/2009WR008856.

1. Introduction

[2] Land water storage plays a fundamental role within the global water cycle and on climate, particularly in regions where the coupling between land surface and the atmosphere is theorized to be important, such as West Africa [*Koster et al.*, 2004]. In this region, land processes related to soil moisture and vegetation have been shown to have an important impact on the development of the summer monsoon by amplifying its response to oceanic forcing [*Giannini et al.*, 2003, 2008]. Monitoring water storage changes over this region is therefore fundamental for better understanding of land-atmosphere processes as well as evapotranspiration-related processes. In addition, given the possible link between soil moisture and the atmosphere, improved knowledge of water storage, which is a relatively slow varying component in the climate system, could lead to improved long-term predictions [*Philippon and Fontaine*, 2002]. Moreover, in West Africa, and particularly in the Sahel, water storage changes directly affect the natural resource availability, and therefore, they have a significant environmental and socioeconomic impact. Water storage is

[1] Géosciences Environnement Toulouse, UMR 5563, CNRS-Université Toulouse III-IRD, Toulouse, France.
[2] Centre National de Recherches Météorologiques, Toulouse, France.
[3] European Centre for Medium-Range Weather Forecasts, Reading, UK.
[4] Dynamique Terrestre et Planétaire, UMR 5562, CNRS-UPS Toulouse III, Toulouse, France.
[5] Centro de Estudios Avanzados en Zonas Aridas, La Serena, Chile.
[6] Laboratoire des Sciences du Climat et de l'Environnement, LSCE/IPSL/CEA-CNRS-UVSQ, Centre d'Etudes de Saclay, Gif-sur-Yvette, France.
[7] Plymouth Marine Laboratory, Plymouth, UK.

0043-1397/11/2009WR008856

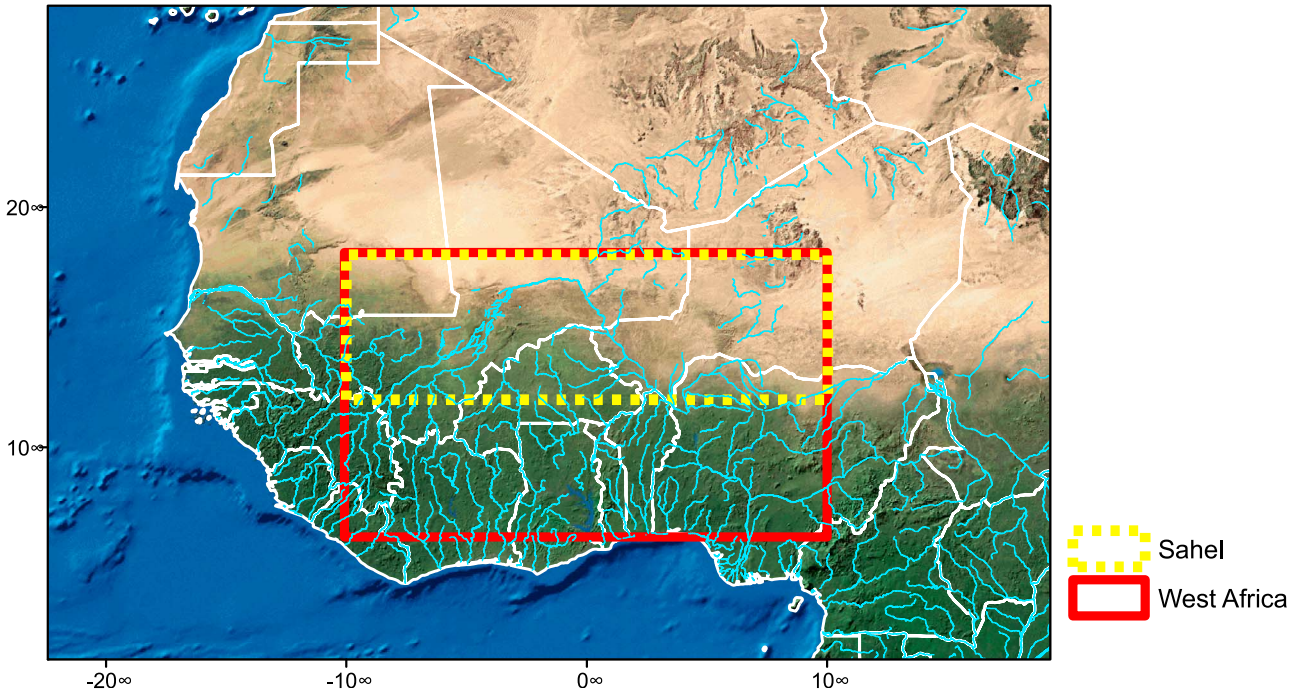

Figure 1. Study area, with the West Africa and Sahel boxes employed in this study overlaid.

a key variable for evaluating the past and present state of natural resources such as water and fodder and for modeling their future development within the context of climate change.

[3] However, direct measurements of land water storage are not readily available at regional and global scales. This is true especially in the Sahel, where monitoring the water budget components is not easy because of the scarcity of in situ measurements, especially in terms of precipitation. Even when local measurements are available, it remains difficult to extrapolate them over larger areas given the relatively large spatial heterogeneity of the main components of the terrestrial water cycle [see, e.g., *Lebel et al.*, 1997]. Moreover, little useful information on water storage can be derived from river discharge measurements since this region is mostly endhoreic; that is, the main West African water basins are not fed by Sahelian waters.

[4] The Gravity Recovery and Climate Experiment (GRACE) satellite mission provides an accurate measurement of terrestrial gravity field variations from which land water storage variations can be derived. As opposed to microwave passive and active spaceborne sensors that can be used to retrieve surface soil moisture in the uppermost few centimeters, GRACE data can be used to estimate water storage variations integrated over the entire water column, including the root zone as well as deeper groundwater reservoirs. The retrieval of the terrestrial water storage (TWS) from the satellite gravity measurements is not straightforward and requires solving an ill-posed inverse problem. Different methods are employed to do this by various research teams [*Chambers*, 2006; *Rowlands et al.*, 2005; *Liu*, 2008; *Bruinsma et al.*, 2010; *Ramillien et al.*, 2005] and provide different GRACE water storage estimates [see, e.g., *Klees et al.*, 2008a].

[5] Since the satellite launch in 2002, GRACE data have been increasingly used for different hydrological applications [e.g., *Ramillien et al.*, 2008a; *Schmidt et al.*, 2008], for example, monitoring of extreme hydrological events [*Chen et al.*, 2009; *Seitz et al.*, 2008; *Andersen et al.*, 2005], evaluating hydrological fluxes such as evapotranspiration [*Rodell et al.*, 2004; *Ramillien et al.*, 2006], and computing atmospheric water vapor convergence [*Swenson and Wahr*, 2006a] and river discharge [*Syed et al.*, 2005] as well as for integrated water budget studies [*Yirdaw et al.*, 2008; *Crowley et al.*, 2006].

[6] Evaluation of the seasonal and interannual variability of the GRACE water storage estimates has been mainly carried out over well-defined water basins at regional or global scales. GRACE water storage products have been compared to in situ measurements using soil moisture networks [*Swenson et al.*, 2008], to well level data combined with hydrological models [*Schmidt et al.*, 2008], and to modeling results [e.g., *Schmidt et al.*, 2006; *Papa et al.*, 2008; *Syed et al.*, 2008; *Schmidt et al.*, 2008; *Klees et al.*, 2008a]. GRACE data have also been used to provide useful information for calibrating and/or improving the water storage simulation in land surface models [*Ngo-Duc et al.*, 2007; *Niu et al.*, 2007; *Güntner*, 2008; *Syed et al.*, 2008; *Alkama et al.*, 2010].

[7] Until recently, only a few GRACE studies have been carried out over West Africa, despite the fact that several global studies included the Niger River basin [e.g., *Papa et al.*, 2008; *Schmidt et al.*, 2008; *Ramillien et al.*, 2008b; *Syed et al.*, 2008; *Ngo-Duc et al.*, 2007]. No extensive evaluation of GRACE water products has been performed for the Sahel and, more generally, for endhoreic areas. Moreover, the capability of GRACE to reproduce the interannual variability of water storage changes over West Africa has not been specifically addressed.

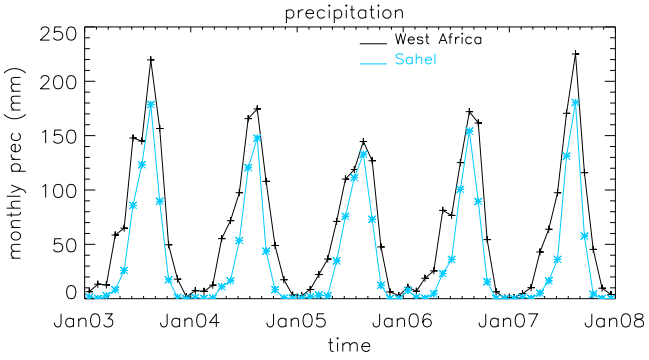

Figure 2. Monthly precipitation (mm) over West Africa and the Sahel by the TRMM data set employed for the ALMIP simulations.

[8] The objective of this work is to better understand the intraseasonal and interannual variability of the water cycle over West Africa and, in particular, the Sahel. This is done by using GRACE TWS products as well as soil moisture derived by an ensemble of land surface models participating in the African Monsoon Multidisciplinary Analysis Land Surface Intercomparison Project (ALMIP) [*Boone et al.*, 2009]. For the time period 2003–2007, satellite product and model outputs are analyzed and compared considering different aspects of the continental water storage: the seasonal cycle (amplitude and phase), the interannual variability during the wet and dry seasons, and the zonal distribution.

[9] The study area is the West African region bordering the Guinean gulf to the south and the Sahara desert to the north (Figure 1). The analysis is carried out over two arbitrary areas: the "West Africa" box between 10°–10°W–10°E and 6°N–18°N and the "Sahel" box between 10°W–10°E and 12°N–18°N.

[10] West Africa is characterized to a good approximation by a zonal distribution of precipitation and land cover. The annual precipitation gradient ranges from about 1000 mm/yr in the Guinean zone to 100 mm/yr to the north of the Sahelian region. The precipitation annual cycle (Figure 2) is driven by the West African monsoon, and it is related to the meridional displacement of the Intertropical Convergence Zone (ITCZ) [*Sultan and Janicot*, 2003]. It reaches 5°N in April and stays in a quasi-stable position until the end of June, then it abruptly shifts during the first half of July to 10°N, where it remains until the end of August. Over the Sahel, the rainy season peaks between July and September. The ITCZ gradually withdraws southward from September to November, and this withdrawal is associated with a sharp precipitation decrease over this region.

[11] The West African hydrological systems are also roughly organized as a function of the latitudinal gradient, with significant water lateral transfers within deeper soil layers in the southern areas and Hortonian systems, characterized by superficial water flow, to the north [*Peugeot et al.*, 1997; *Braud et al.*, 1997]. Southern areas are mostly exorheic with considerable sheet runoff. The hydrological system become progressively endhoreic going northward, where, depending on the soil properties, endhoreic sandy soils alternate with smaller areas characterized by concentrated runoff. The Sahel is dominated by large old sedimentary basins consisting of either deep fossil aquifers or less deep, more or less fragmented, actively recharged aquifers which are affected by minor seasonal fluctuations and decadal trends [*Favreau et al.*, 2009]. The southern half of the West African box is dominated by the African Shield, with shallow fragmented aquifers which have variations that follow the seasonal pattern of rainfall and river drainage.

[12] The vegetation gradient follows the precipitation pattern: going from south to north, the dominant vegetation consists of forest, savannah and parkland, and grassland and open shrub lands. Crops and fallows are also present, and they are scattered throughout the study region.

[13] The largest river in the Sahel is the Niger, but the majority of the Sahel box is endhoreic and does not feed the Niger River [*Descroix et al.*, 2009]. The runoff seasonal evolution is delayed compared to the precipitation seasonal cycle. The maximum runoff enters and exits the Sahel box in September, and the river flow decreases after the rain season at a slower rate than precipitation. The Inner Niger delta, an area of swamps and small lakes in the Sahelian region in Mali, typically floods during the wet season and is subject to intense evaporation, further delaying the Niger discharge seasonal cycle.

2. Data and Methods

[14] The GRACE satellite mission, managed by NASA and the German Aerospace Center, has been collecting data since mid-2002. Estimates of the Earth's gravity field produced by GRACE can be used to infer changes in mass at and below the surface of the Earth, including the oceans, the polar ice sheets, the land water storage (surface water, soil moisture, snow, and groundwater) and the solid Earth. To extract land water storage changes on a given region of the Earth, two issues need to be addressed. (1) The contributions of atmospheric, oceanic, and solid Earth mass variations need to be separated from the hydrological signal, which generally requires the employment of background models. (2) The TWS signal over a given region of the Earth needs to be separated from contaminations coming from a different region, such as the water storage variability in a neighboring area or ocean.

[15] In this study, six different GRACE products (Table 1) are employed and are briefly described below.

[16] 1. Three monthly land water solutions (RL04) are provided by the GeoForschungsZentrum (GFZ); the Jet Propulsion Laboratory (JPL), California Institute of Technology; and the Center for Space Research (CSR), University of Texas at Austin, with a spatial resolution of 400 km (available at ftp://podaac.jpl.nasa.gov/tellus/grace/monthly). These three data sets are processed as reported by *Chambers* [2006]. Each monthly gravity field is represented by a set of spherical harmonic (Stokes) coefficients, developed to degree and order 60. CSR, GFZ, and JPL use different algorithms to compute gravity field harmonic coefficients from the raw GRACE observations, although they have agreed to use similar background models for the ocean and the atmosphere. Spatial averaging, or smoothing, of GRACE data is commonly used to reduce the anisotropic noise, which manifests itself in strong north–south stripes. Systematic errors causing the longitudinal stripes, identified by correlations between spherical harmonic coefficients of like parity within a particular spectral order, are removed using the destriping

Table 1. GRACE Products Employed in This Study

Product Name	Spatial Grid	Spatial Resolution	Temporal Frequency	Time Span
GFZ-v 04	1° × 1°	400 km	1 month	Oct 2002–Apr 2008 (missing Jan 2003, Jun 2003, Jan 2004, Sept 2004[a])
JPL-v 04	1° × 1°	400 km	1 month	Aug 2002–Apr 2008 (missing Jan 2003, Jun 2003, Jan 2004)
CSR-v 4.1	1° × 1°	400 km	1 month	Sep 2002–Apr 2008 (missing Jun 2003, Jan 2004)
DEOSS DMT V 1	1° × 1°	400 km	1 month	Feb 2003–Dec 2007 (missing Jun. 2003)
CNES-GRGS v 2	1° × 1°	400 km	10 days	Aug 2002 to May 2008
GSFC-mascons	4° × 4°	4° × 4°	10 days	Apr 2003 to Apr 2007

[a]Removed because of aliasing problems.

method described by *Swenson and Wahr* [2006b]. After destriping, the signal can be further smoothed using a Gaussian filter of a certain radius. For the comparison to the ALMIP results, in this study we employ the destriped but unfiltered solutions. However, solutions smoothed with a Gaussian filter of radius equal to 500 and 300 km are also analyzed in section 2.1.1 in order to better investigate the effects of filtering.

[17] 2. The DEOS Mass Transport Model (DMT) monthly solutions by the University of Delft (available at http://www.lr.tudelft.nl). They are also based on the decomposition into spherical harmonic Stokes coefficients but to degree and order 120. The details of the computation of monthly solutions and corresponding covariance matrices are given by *Liu* [2008]. The series of monthly solutions is postprocessed by applying statistically optimal Wiener filters on the basis of full signal and noise covariance matrices instead of a Gaussian filter. The signal variances and solutions are computed iteratively, according to the scheme described by *Klees et al.* [2008b].

[18] 3. The level-2 GRGS-EIGEN-GL04 10 day models provided by Centre National d'Études Spatiales (CNES) are derived from GRACE GPS and K band range rate data and from LAGEOS-1/2 satellite laser ranging data [*Bruinsma et al.*, 2010] (available at http://grgs.obs-mip.fr/index.php/fre/Donnees-scientifiques/Champ-de-gravite/grace/release02). These gravity fields are expressed in terms of normalized spherical harmonic coefficients from degree 2 up to degree 50 using a stabilization approach without additional filtering. We use the TWS 10 day grids with a spatial resolution of 1° × 1° from January 2003 to December 2007.

[19] 4. The 10 day land water solutions from the NASA Goddard Spaceflight Center (GSFC), with a spatial resolution of 4° × 4°, are available for the period April 2003 to April 2007 at http://grace.sgt-inc.com/. The data are processed with an approach based on a local time-dependent mass recovery using mass concentrations blocks (mascons) [*Rowlands et al.*, 2005] rather than using global basis functions such as spherical harmonics. The formulation for mascon solutions exploits the fact that a change in potential caused by adding a small uniform layer of mass over a region at a time t can be represented as a set of (differential) potential coefficients which can be added to the mean background field. Mascons can be located in space, and hence, short wavelength errors (e.g., due to ocean tides) should not leak into land areas, although spatial constraints are imposed on neighboring 4° × 4° pixels.

[20] In our study, the water storage anomalies (reported in mm) have been recentered for each solution by removing the mean over the 2003–2006 common period.

2.1. Filtering and Leakage

[21] Several recent studies have shown that GRACE data over the continents provide information on the total land water storage with an accuracy between 15 and 30 mm of liquid water thickness equivalent [*Schmidt et al.*, 2006; *Llubes et al.*, 2007; *Klosko et al.*, 2009], depending on the region considered. GRACE water storage estimates at a given location are affected by data processing, which requires a compromise between maximizing spatial resolution and reducing noise.

[22] This is done following different approaches, such as (1) truncating the harmonical series computation at a given degree (50, 60, or 120: the lower the degree, the greater the smoothing) as done for all the products considered here except the mascons (CSR,JPL, and GFZ truncating at degree 60, CNES truncating at degrees 2–50, and DMT truncating at 120); (2) applying smoothing filters, such as the Gaussian filtering with the radius of 300 and 500 km used by the CSR, JPL, and GFZ postprocessed solutions or the optimal Wiener filter used in the DMT model; (3) employing stabilization approaches such as that used for the CNES solution; and (4) imposing spatial constraints as done for the mascon solutions.

[23] All of these approaches make the water storage estimates in a given region biased and sensitive to mass changes outside the region of interest (leakage). Leakage is composed of two mechanisms: (1) leakage of signal from the target area to the surroundings (leakage out) and (2) leakage of signal from the surroundings into the target area (leakage in). In this paper, we employ the term leakage to mean both mechanisms (leakage in and out), even if sometimes this term is used to described the second mechanism only. A survey of different methods employed to take into account leakage effects can be found in work by *Longuevergne et al.* [2010]. *Chen et al.* [2005] showed that if temporal water storage variations are homogeneous over a sufficiently large area, leakage in and out may partially cancel each other, minimizing the overall leakage effect. On the contrary, leakage effects are expected to have the highest impact when mass changes inside the study region are in opposition of phase with mass changes outside it. For basins surrounded by areas with smaller storage variations (oceans and deserts) the effects of leakage should therefore make the effective water storage underestimated.

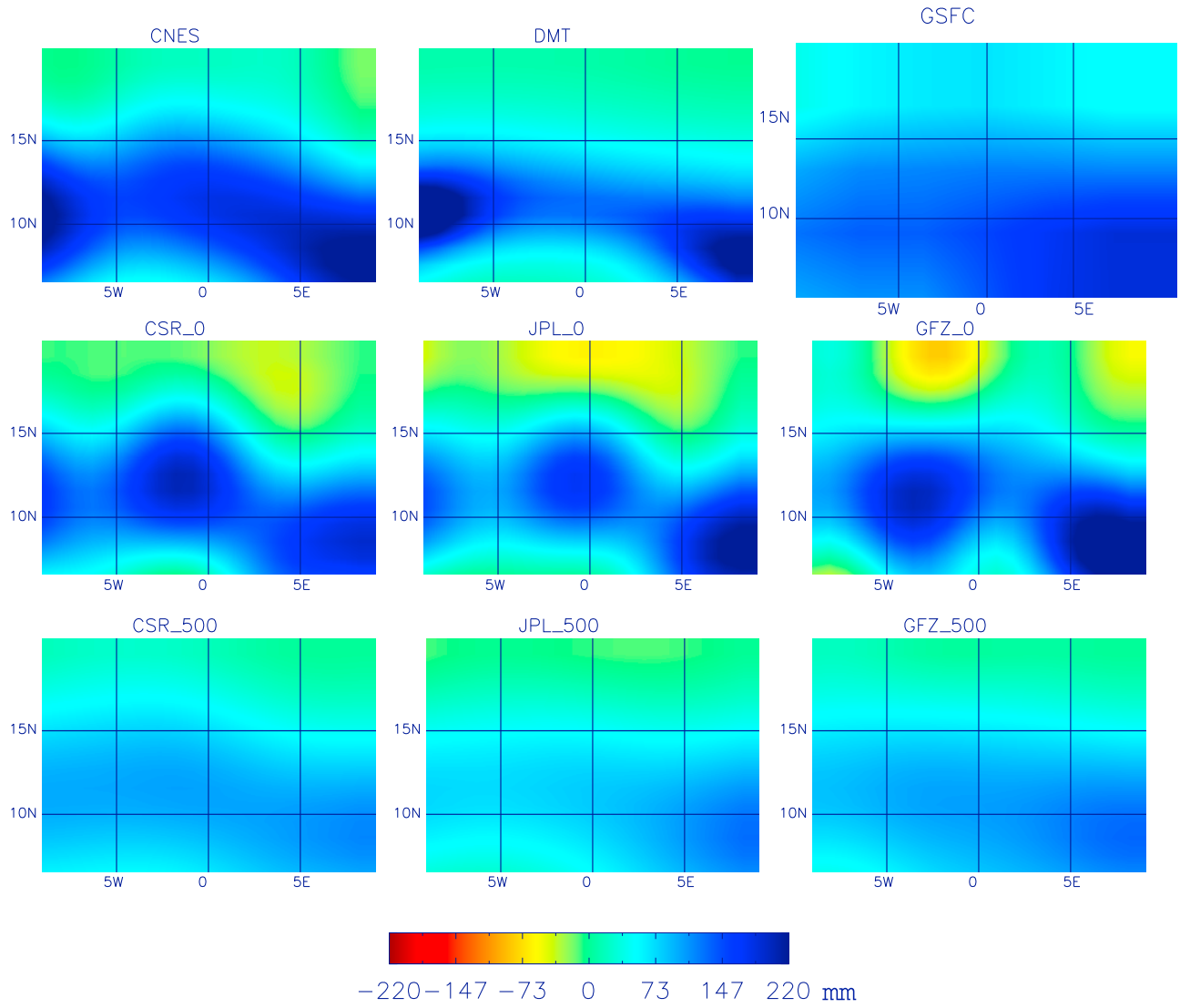

Figure 3. Spatial distribution of water storage anomalies (mm) over the West Africa study region for all the GRACE products during September 2006.

[24] Figure 3 shows, for each product, the spatial distribution of water storage anomalies in September, the month of the maximum soil water over West Africa. To illustrate the impact of using a Gaussian filter in the postprocessing, CSR, JPL, and GFZ solutions smoothed by a Gaussian filter of 500 km radius are also shown. All GRACE estimates indicate a maximum, more or less pronounced, at the southeast corner of the study area and another maximum at a latitude of about 12°N but at different longitudes for different products. In addition, CSR, JPL, and GFZ at 500 km appear much smoother than the same unfiltered solutions. However, the latter solutions show the effects of residual longitudinal stripes not completely eliminated by the destriping process by *Swenson and Wahr* [2006b]. Alternative destriping methods [*Frappart et al.*, 2011; *Klees et al.*, 2008b; *Kusche*, 2007], which are more efficient for equatorial areas, may be applied. However, in this study, these effects are not a major problem given that we analyze water storage changes averaged over a sufficiently large longitudinal domain.

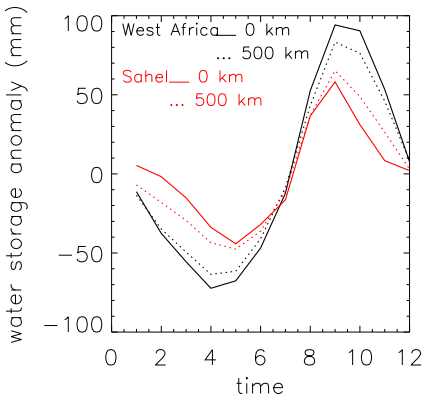

Figure 4. Seasonal cycle (multiannual mean over the study period 2003–2007) for CSR, JPL, and GFZ solutions unsmoothed and smoothed by a Gaussian filter of 500 km.

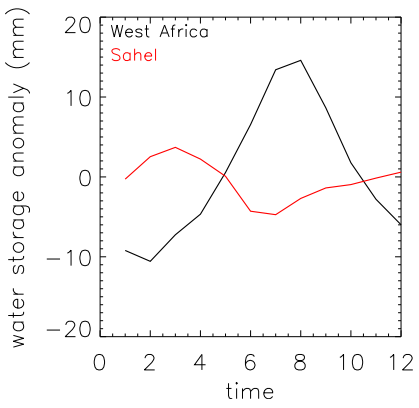

Figure 5. Leakage correction for CSR solutions over West Africa and the Sahel.

[25] Regarding the seasonal dynamics, Figure 4 shows the comparison between the CSR, JPL, and GFZ solutions (multiproduct mean) postprocessed by a Gaussian filter with a 500 km radius and the corresponding solutions without any Gaussian filtering. Over the West African box, filtered data show a lower dynamic than that shown by the unfiltered data, which is consistent with the geographic configuration, West Africa being surrounded by areas with small seasonal dynamics (ocean and Sahara desert). Conversely, for the Sahel box, the 500 km Gaussian filter slightly increases the seasonal dynamics. This implies that contamination from the Soudanian area, located to the south of the Sahel box, more than compensates for the damping effect from the Sahara desert at the northern border. Differences between the monthly TWS values of smoothed and unsmoothed solutions are no more than 10–15 mm for both

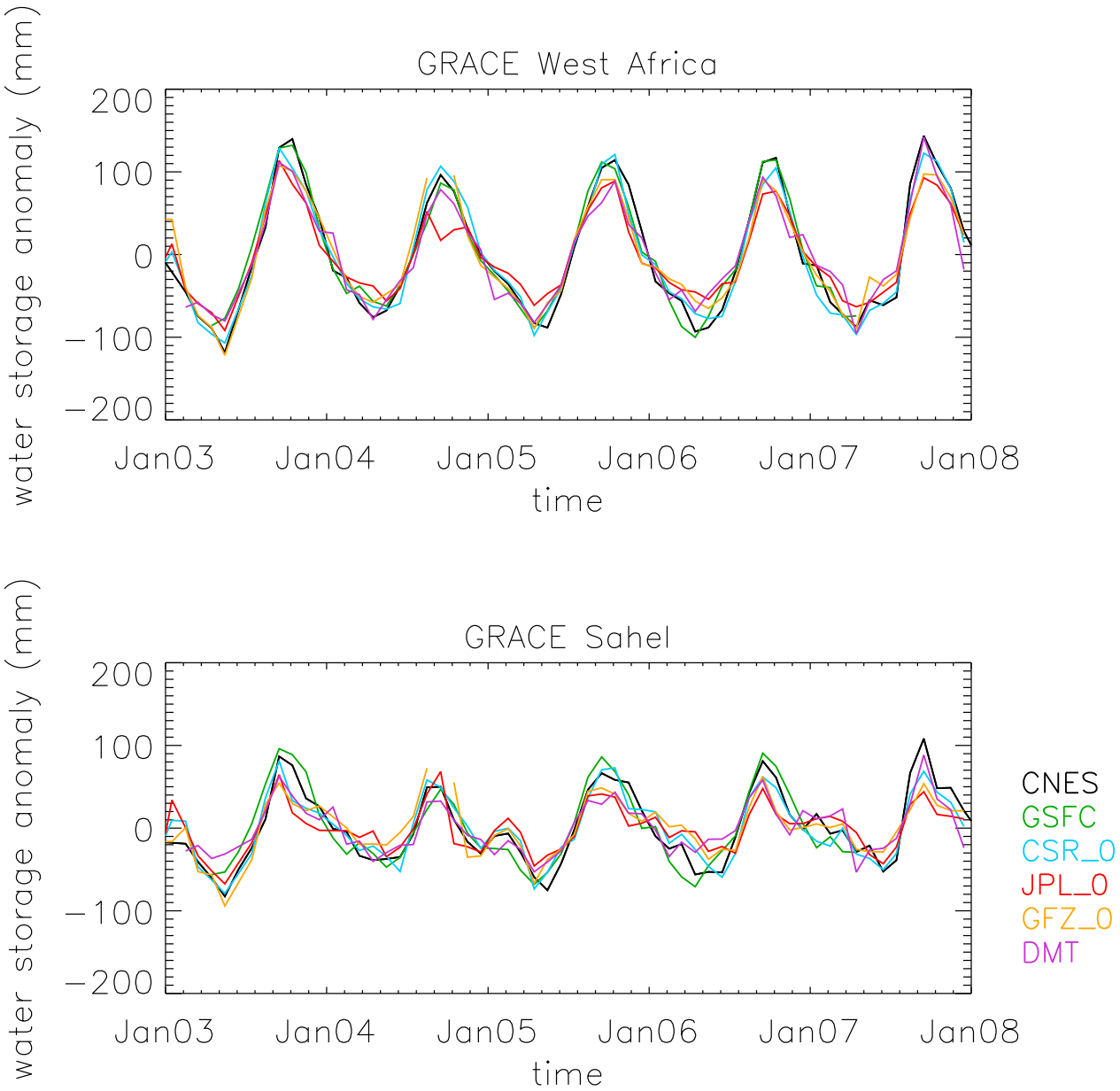

Figure 6. Water storage changes for the six different GRACE solutions employed in this study, spatially averaged over the (top) West Africa and (bottom) Sahel boxes.

Table 2. Land Surface Models Participating in ALMIP-Exp3[a]

Model Acronym	Institute[b]	Recent Reference	ALMIP Configuration
HTESSEL	ECMWF, Reading, UK (G. Balsamo)	*Balsamo et al.* [2009]	4L, 6 tiles, 1E, SV: ECMWF
ORCHIDEE -CWRR	IPSL, Paris (P. de Rosnay)	*d'Orgeval et al* [2008], *de Rosnay et al.* [2002]	11L, 13 tiles, 1E, SV: ECOCLIMAP
ISBA	CNRM, Toulouse, France (A. Boone)	*Noilhan and Mahfouf* [1996]	3L, 1 tile, 1E, SV : ECOCLIMAP
JULES	CEH, Wallingford, UK (P. Harris)	*Essery et al.* [2003]	4L, 9 tiles, 2E, SV: ECOCLIMAP
SETHYS	CETP/LSCE, France (S. Saux-Picart and C. Ottlé)	*Saux-Picart et al.* [2009]	3L, 12 tiles, 2E, SV: ECOCLIMAP
NOAH	CETP/LSCE (NCEP) (B. Decharme and C. Ottlé)	*Chen and Dudhia* [2001], *Decharme* [2007]	7L, 12 tiles, 1E, SV: ECOCLIMAP
CLSM	UPMC, Paris (S. Gascoin and A. Ducharne)	*Koster et al.* [2000] *Gascoin* [2009]	3L, 5 tiles, 1E, SV: ECOCLIMAP
SSiB	LETG, Nantes, France, and UCLA, Los Angeles, USA, (I. Poccard-Leclercq)	*Xue et al.* [1991]	3L, 1 tile, 2E, SV: SSiB
SWAP	IWP, Moscow (Y. Gusev and O. Nasonova)	*Gusev et al.* [2006]	3L, 1 tile, 1E, SV: ECOCLIMAP

[a]The names of the people who performed the simulations appear in parentheses after the institute name. The model configuration used for ALMIP is shown in the last column, where L represents the number of vertical soil layers, E represents the number of energy budgets per tile, and SV corresponds to the soil-vegetation parameters used. Tile refers to the maximum number of completely independent land surface types permitted within each grid box.

[b]IPSL, Institut Pierre-Simon Laplace; CNRM, Centre National de Recherches Météorologiques; CEH, Centre for Ecology and Hydrology; CETP, Centre de Recherches en Physique de l'Environnement Terrestre; LSCE, Laboratoire des Sciences du Climat et de l'Environnement; UPMC, Université Pierre et Marie Curie; LETG, Littoral-Environnement-Télédétection-Géomatique; UCLA, University of California, Los Angeles; IWP, Institute of World Policy.

regions but are more significant at about 10°, where CSR, JPL, and GFZ unfiltered solutions are more coherent with the other solutions analyzed (CNES, DMT, and GSFC) than the CSR, JPL, and GFZ solutions postprocessed using a Gaussian filter (not shown).

[26] Leakage resulting from the combined effects of Gaussian filtering, destriping, and truncating the harmonical series can be estimated from hydrological models, as done, for example, by *Klees et al.* [2007] and by Swenson (http://grace.jpl.nasa.gov/data/gracemonthlymassgridsoverview/), who propose correcting factors to account for this. This is estimated here for the CSR, JPL, and GFZ solutions following the method by Swenson that calculates a correcting factor on a 1° grid basis by using a global simulation of land hydrology. The simulated TWS field underwent the same processing as the RL04 data: spherical harmonical expansion, truncation to degree 60, and destriping. The data were then postprocessed using a 300 km Gaussian filter and then were regressed against the original TWS. The regression slope can then be used as a correction factor for the GRACE data. This correction, accounting for leakage out and leakage in, is shown in Figure 5 for the West Africa and the Sahel boxes. It has very similar effects to those attributed to the application of the Gaussian filter alone (Figure 4), with the GRACE seasonal dynamics enhanced over West Africa and reduced for the Sahel box. A similar calculation with another hydrological model following the method by *Ramillien et al.* [2008b] (not shown) resulted in a slightly higher leakage over the Sahel box.

[27] In conclusion, the above estimates of leakage errors imply that, for global solutions, water storage changes are probably underestimated for the West Africa box, whereas they may be slightly overestimated for the Sahel box. A complete error budget should also address the data and inversion errors, which are not known precisely. In this analysis, we do not apply explicit corrections to account for leakage effects given that they are dependent on hydrological models and on the methodology followed to calculate them. Our approach is therefore to intercompare the different GRACE solutions to have a rough idea of GRACE processing errors.

[28] The temporal evolution of the TWS by all the GRACE products considered, spatially averaged over the West African and the Sahelian boxes (given its coarser resolution, the GSFC product has been averaged over slightly larger boxes, with latitudes between 4°N and 20°N for West Africa and between 12°N and 20°N for the Sahel and longitudes between 12°W and 12°E), is shown in Figure 6. The six products are quite consistent regarding their temporal evolutions, with water storage maxima generally found in September and minima found in April (West Africa) and May (Sahel). A temporal shift is sometimes observed with respect to the dates at which the maxima and minima are reached: this is not systematic for a given product, and it is more important for the dates of the water storage minima, for which the shift can be up to 2 months (as, for example, over the Sahel in 2007). In terms of the amplitudes of the seasonal water storage changes (for each year, the difference between the maximum and minimum value), the six GRACE products show significant differences, with the CNES and CSR solutions generally higher and GFZ lower than the other solutions. Year to year variations are also observed among the different solutions.

2.2. ALMIP Models

[29] The ALMIP model intercomparison [*Boone et al.*, 2009] was carried out by running different state-of-the-art land surface models using the same forcing database, which consists of atmospheric state variables, precipitation, and incoming radiative fluxes. The atmospheric state variables were derived from European Centre for Medium-Range

Table 3. Water Budget Components by the ALMIP Land Surface Models Over West Africa and the Sahel[a]

	Year				
	2003	2004	2005	2006	2007
	West Africa				
Precipitation (mm/yr)	894	769	698	740	791
Evaporation (mm/yr)	639	619	591	585	575
Surface runoff (mm/yr)	67	52	44	49	61
Drainage (mm/yr)	164	110	77	103	145
	Sahel				
Precipitation (mm/yr)	535	404	449	433	433
Evaporation (mm/yr)	437	362	381	377	361
Surface runoff (mm/yr)	35	24	26	23	28
Drainage (mm/yr)	58	32	33	29	40

[a]For the ensemble of the ALMIP models considered, mean values are reported.

Weather Forecasts (ECMWF) short-term forecast data, while downwell radiative fluxes were a mix of ECMWF and Land Surface Analysis Satellite Applications Facility estimates.

[30] For the simulation of the different components of the water budget, the most crucial forcing variable is precipitation. In this study, we used the simulations forced by the Tropical Rainfall Measurement Mission (TRMM) precipitation product 3B-42 [*Huffman et al.*, 2007] (see Figure 2). Nine different models made for climate or numerical weather prediction (for example, SSIB, NOHA, HTESSEL, ISBA, and ORCHIDEE) or more hydrologically based models (for example, CLSM) participated in this intercomparison (Table 2). These models have different degrees of complexity in terms of the representation of the water budget variables, such as the number of vertical soil layers and the soil depth over which vertical water transfers are simulated (for more details see *Boone et al.* [2009]). Among the ALMIP models, CLSM is the only model including a

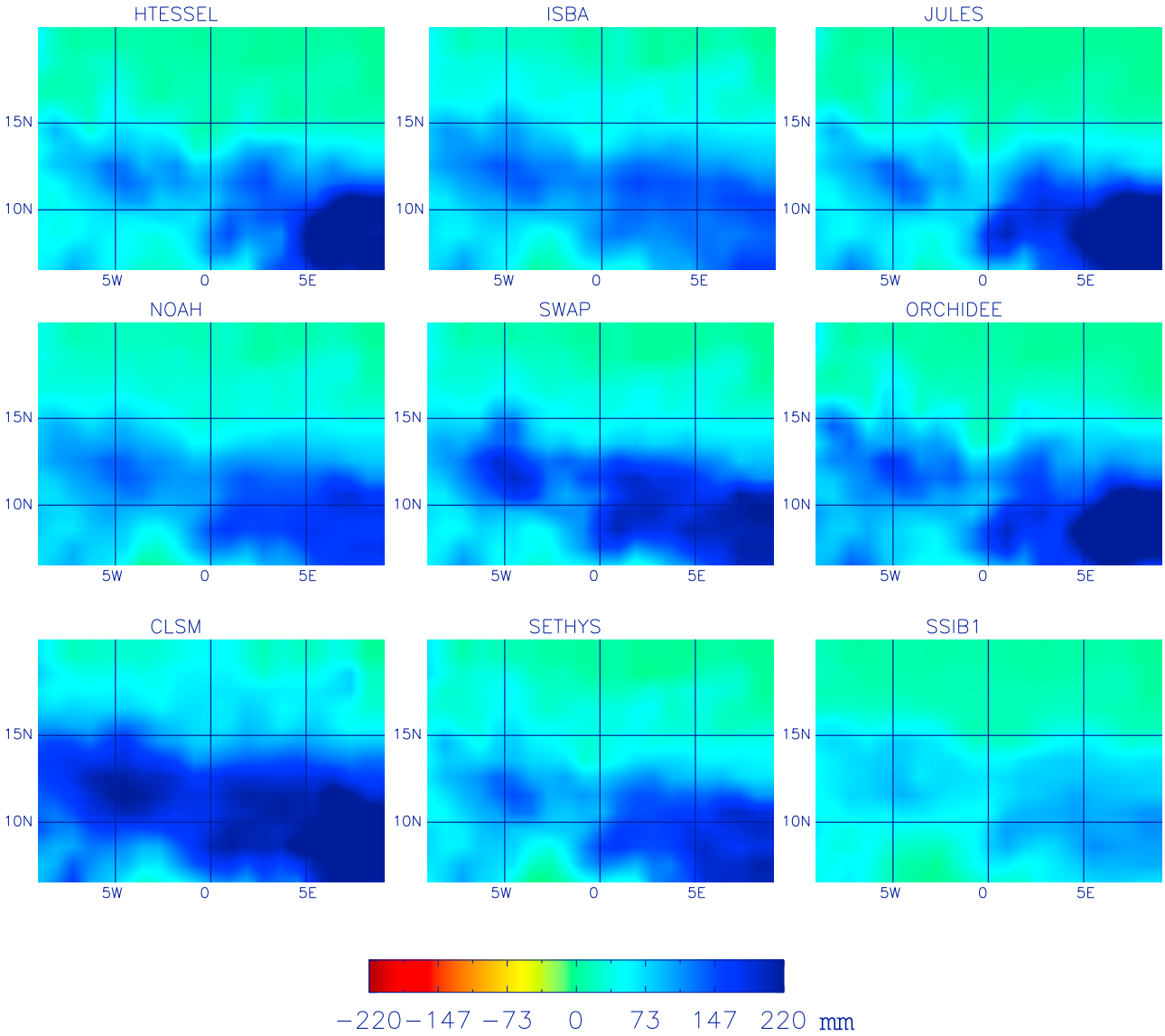

Figure 7. Spatial distribution of water storage anomalies (mm) over the West Africa study region for all the ALMIP models analyzed during September 2006.

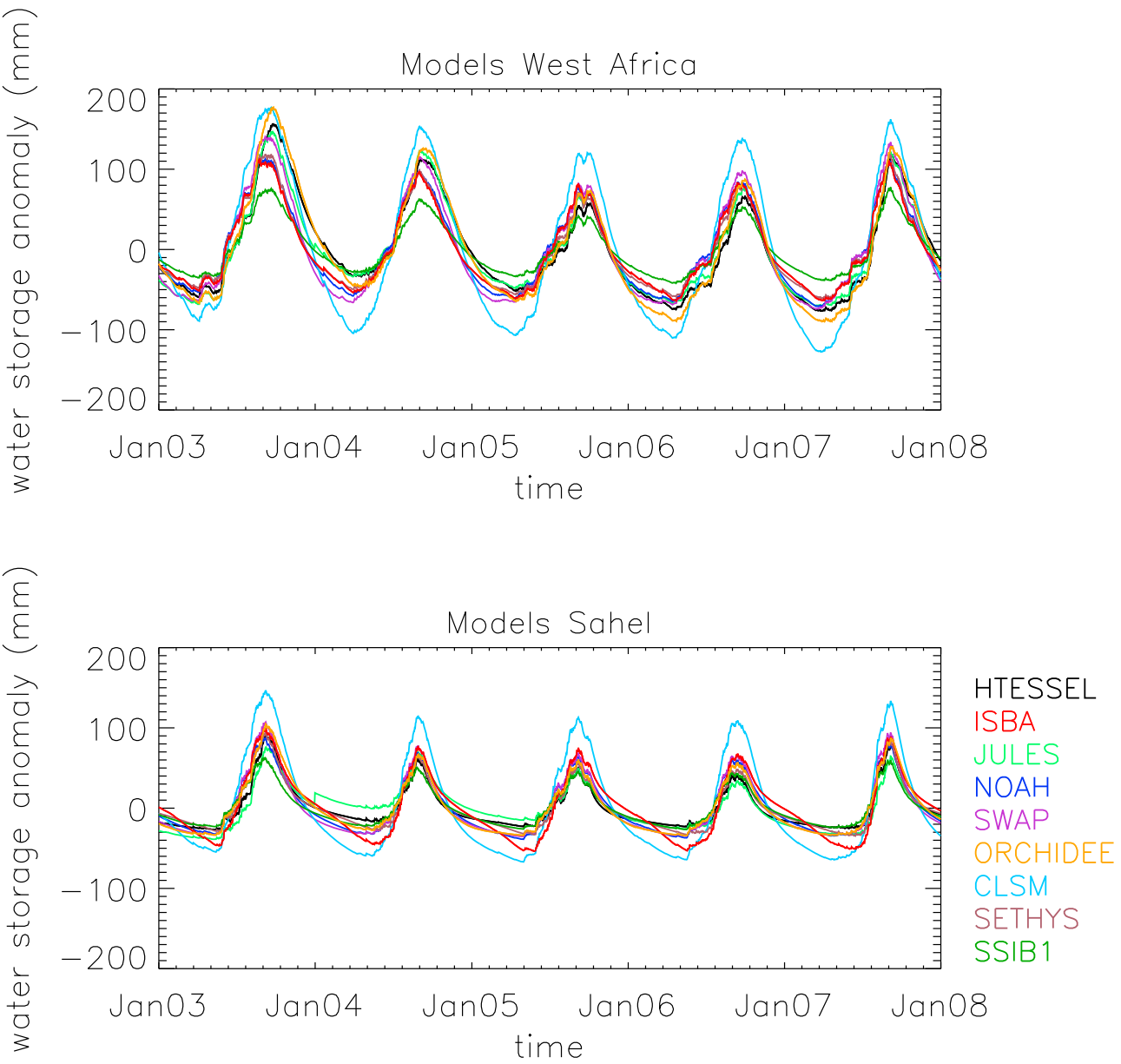

Figure 8. Simulated water storage changes for the nine different models employed in this study, spatially averaged over the (top) West Africa and (bottom) Sahel boxes.

representation of a saturated area following the TOPMODEL concept. Land surface parameters concerning soil and vegetation are taken form the ECOCLIMAP database for all models except for HTESSEL and SSIB.

[31] The time change in soil moisture, ΔS, vertically integrated over all of the soil layers, is the output variable considered in the following analysis for comparison with GRACE water storage change. It is related to the other water budget variables (input precipitation, P; evapotranspiration, E; and total runoff, including surface runoff and drainage, R, in mm/h) by the following equation:

$$\frac{dS}{dt} = P - E - R.$$

ΔS is calculated in the ALMIP experiment over a time interval of 3 h. Mean annual values for the variables on the right-hand side of the above equation are reported in Table 3. Simulated evapotranspiration is very significant over the Sahel, accounting for 85% of input precipitation on average (multimodels average for the whole study period). Total runoff is much less, with surface runoff accounting for 6% and drainage for 8.5% of input precipitation. Total runoff is more significant in the southern part of the study area, where it is 30% of input precipitation, while evapotranspiration accounts for 70% of input precipitation between 6°N and 12°N. However, the partitioning between evapotranspiration and total runoff is quite variable among different models: over the West Africa region, average yearly simulated evapotranspiration ranges from a minimum value of 482 mm/yr for the SSIB1 model to a maximum of 677 mm/yr for the HTESSEL model. Total runoff ranges from a minimum value of 95 mm/yr for the HTESSEL model to a maximum of 317 mm/yr for the SSIB1 model.

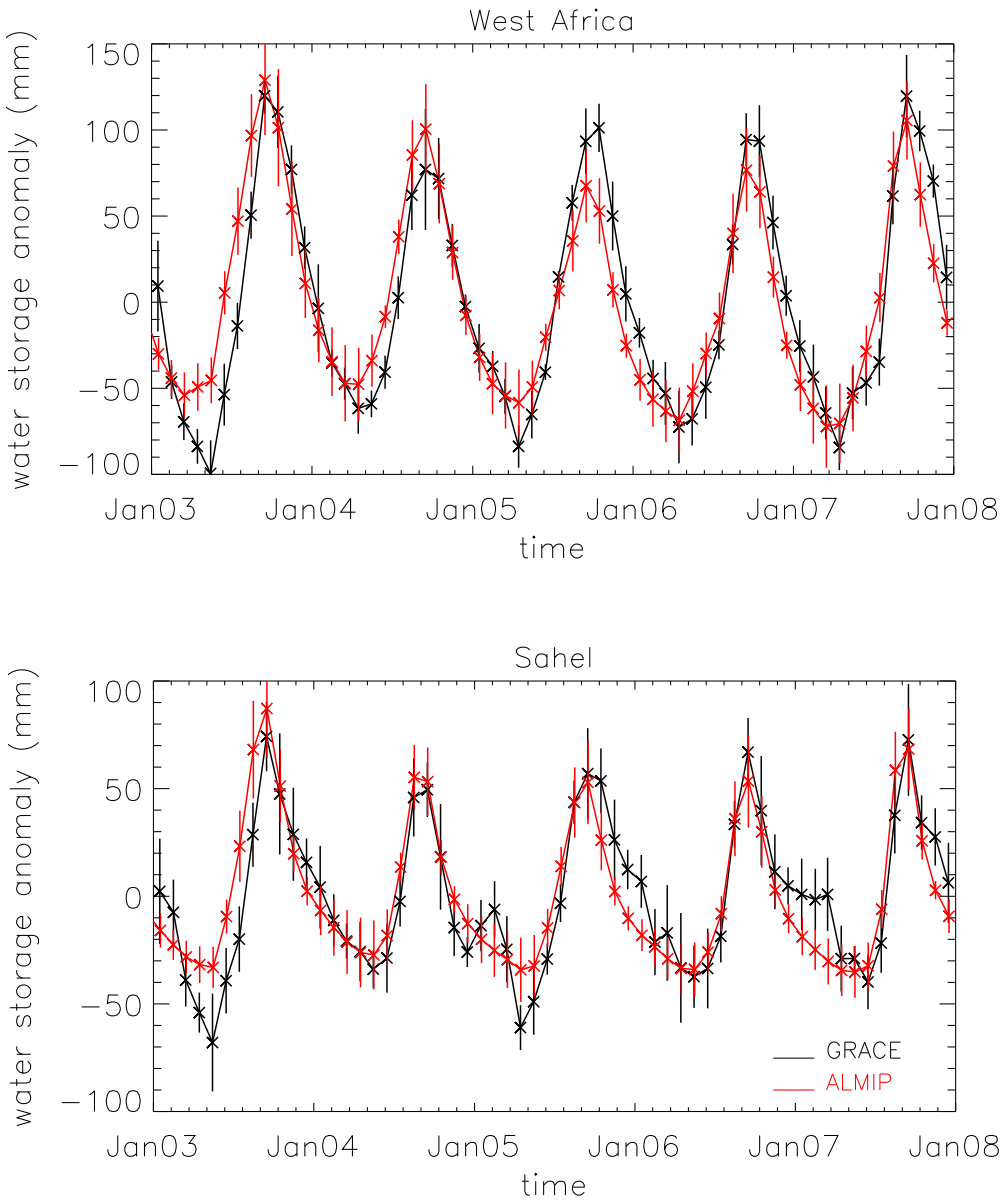

Figure 9. Temporal evolution of GRACE (multisolutions mean and standard deviation) and ALMIP (multimodels mean and standard deviation) water storage variations for (top) West Africa and (bottom) the Sahel.

As was done for the GRACE products, ΔS was integrated over time to obtain monthly soil moisture and then was transferred to anomalies by removing the mean over the 2003–2006 period.

[32] The spatial distribution of soil moisture anomalies for the different ALMIP models in September is shown in Figure 7. All models have a soil moisture maximum to the southeast corner of the study area, and this is more evident for HTESSEL, ORCHIDEE, and JULES than for the other models. Another area of high soil moisture, more or less pronounced, is found by the majority of models at about 12°N, 5°W. Figure 8 shows the temporal variability of modeled water storage spatially averaged over the West Africa and the Sahel boxes for the nine land surface models considered. The temporal changes are very coherent among the different models, and the dry and wet phases are well represented. This is perhaps not surprising since soil moisture changes are determined primarily by the precipitation events that are the same for all models. However, large differences among the model simulations can be observed during the drying phase following the rainy season. Differences in the parameterizations employed by different land surface models are indeed enhanced in this period compared to the wetting phase, when the water storage simulation is more constrained by the input precipitation. Significant differences of soil moisture seasonal amplitudes among different models are also observed.

3. Results

[33] In this section, the spatial and temporal distribution of water storage anomalies by GRACE and soil moisture anomalies by ALMIP are analyzed. Given the scatter among different GRACE water storage estimations as well as

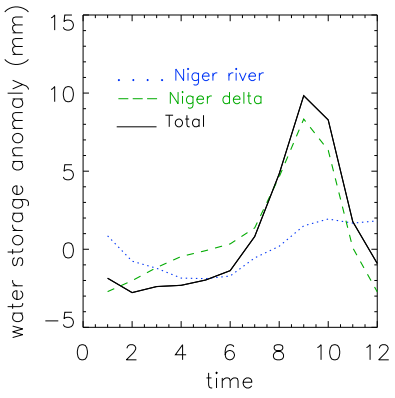

Figure 10. Water storage contribution from the Niger River (water in the river itself, water in the delta, and total) to water storage in the Sahel box.

among different model results, the comparison between GRACE products and ALMIP results does not allow the determination of the "best" GRACE products or the "best" land surface model. Therefore, in the following analysis, results are first presented as mean and standard deviation values for the six GRACE products compared to mean and standard deviation values for the nine ALMIP models considered.

[34] Figure 9 shows the temporal evolution of the mean GRACE and the mean ALMIP water storage anomalies over the 2003–2007 period. A general agreement is found between satellite and model estimations: the wet and dry phases are distinguished well in both cases, and water storage mean amplitudes are quite similar. The overall agreement between GRACE and the models is worse during the dry season: GRACE products show a strong interannual variability that is not observed for the ALMIP models in the dry season. Moreover, a water storage increase during the dry season (January–March) is sometimes observed in the GRACE data, particularly in 2005 but also in 2007 and to a lesser extent in 2006. This increase, detected by all of the GRACE products (Figure 6), is unlikely related to the data processing methodology, but its causes remain unclear.

[35] The comparison between satellite and model outputs has to be carried out carefully since the two estimates are not completely equivalent. Water storage estimates by GRACE do take into account soil water integrated over the entire soil depth and therefore include aquifers as well as surface water contained within river beds and floodplains. In the land surface models employed here, the entire "hydrologically active" soil depth is represented by a shallow soil reservoir. In addition, there is no water transfer between adjacent cells, and drainage through the deepest soil limit is lost. No explicit treatment of river water and floodplains is taken into account in this study. The comparison is therefore valid if these effects are not significant over the study area.

[36] As detailed in section 3.1, for the Sahel box, we have calculated the contribution of water in the Niger River (the largest river of the Sahel box) and in the Niger delta to the seasonal variations of equivalent water height. The effects of aquifers and the water table are much more difficult to quantify given the scarcity of information of these variables at a regional scale and the large heterogeneity of underground systems in West Africa. In this sense, GRACE may provide missing information that is otherwise difficult to quantify. If all the other sources of discrepancies are accounted for, one can argue that the differences between GRACE and ALMIP give an indication of water table variability.

3.1. Niger River and Niger Delta Contribution

[37] The Niger River loses water through evaporation when flowing in the Sahelian zone because of the large floodplain known as the Mali wetland or the Niger inner delta and also because a large part of the basin consists of endhoreic systems, which do not contribute water to the river [*Descroix et al.*, 2009]. Water mass variations have been estimated using satellite altimetry data for the Niger

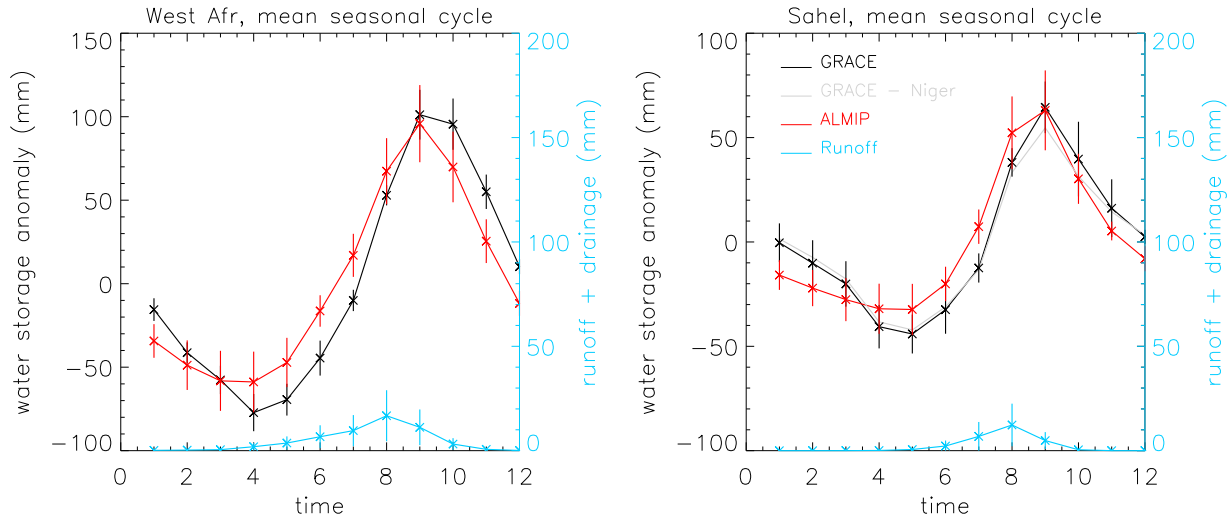

Figure 11. Water storage mean seasonal cycle over the period 2003–2007 for GRACE (multisolutions mean and standard deviation) and ALMIP (multimodels mean and standard deviation) in (left) West Africa and (right) the Sahel. The mean total runoff by ALMIP is also shown in blue. The gray curve in the right-hand plot represents the GRACE water storage without the Niger river contribution (Figure 10).

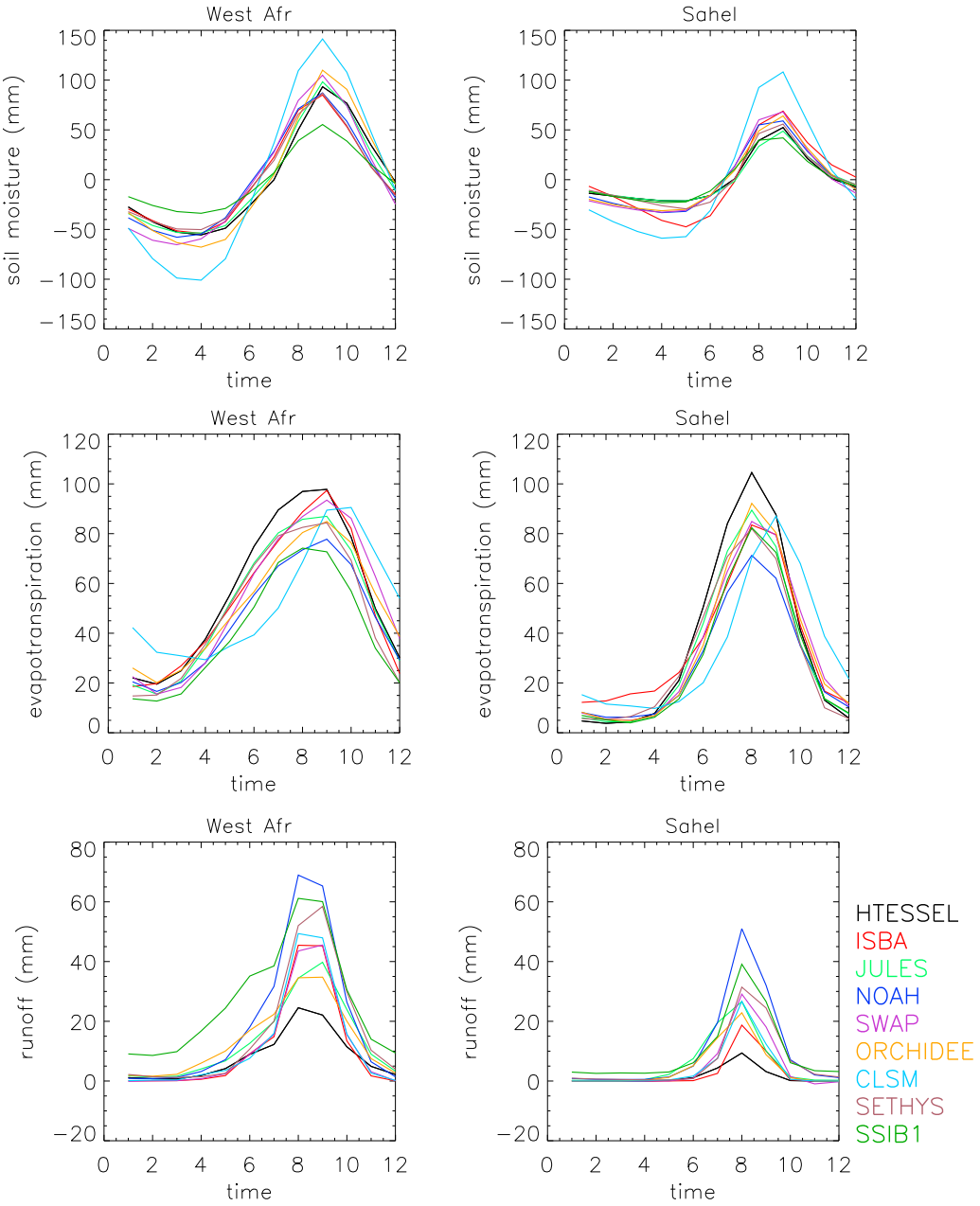

Figure 12. Soil moisture, evaporation, and total runoff (runoff plus drainage) mean seasonal cycle over the period 2003–2007 for the different ALMIP models.

River and from literature for the Niger delta. As detailed in Appendix A, records of 12 altimetry-derived water levels from the Hydroweb Web site (http://www.legos.obs-mip.fr/en/soa/hydrologie/hydroweb/) based on measurements from TOPEX/POSEIDON, Jason-1, ERS-2, ENVISAT, and GFO have been combined with estimates of the river width to derive variations in the river water mass. For the inner delta, the mass of water has been estimated by the difference in river discharge at Dire (outlet) and Douna and Kirango (upstream) from the Global Runoff Data Center (http://www.grdc.sr.unh.edu/), subtracting evaporation losses within the delta (see Appendix A).

[38] Figure 10 shows the Niger River and Niger delta TWS (mm) anomaly for the Sahel box. The main contribution is due to the delta, with a seasonal amplitude of −4–6 mm, while the river water mass varies between -2 and 2 mm. Because of the delay caused by the slow water progression in the floodplain, the Niger flood peak shifts from August to December when flowing in the Sahel box, which attenuates the seasonal cycle of the total mass variation. The contribution of the other rivers in the Sahel box is expected to be, at most, of the same magnitude as the Niger River, with a seasonal cycle of a few millimeters or less.

3.2. Seasonal Cycle

[39] The mean seasonal cycle, calculated as the mean over the period 2003–2007 for each month, is plotted in Figure 11.

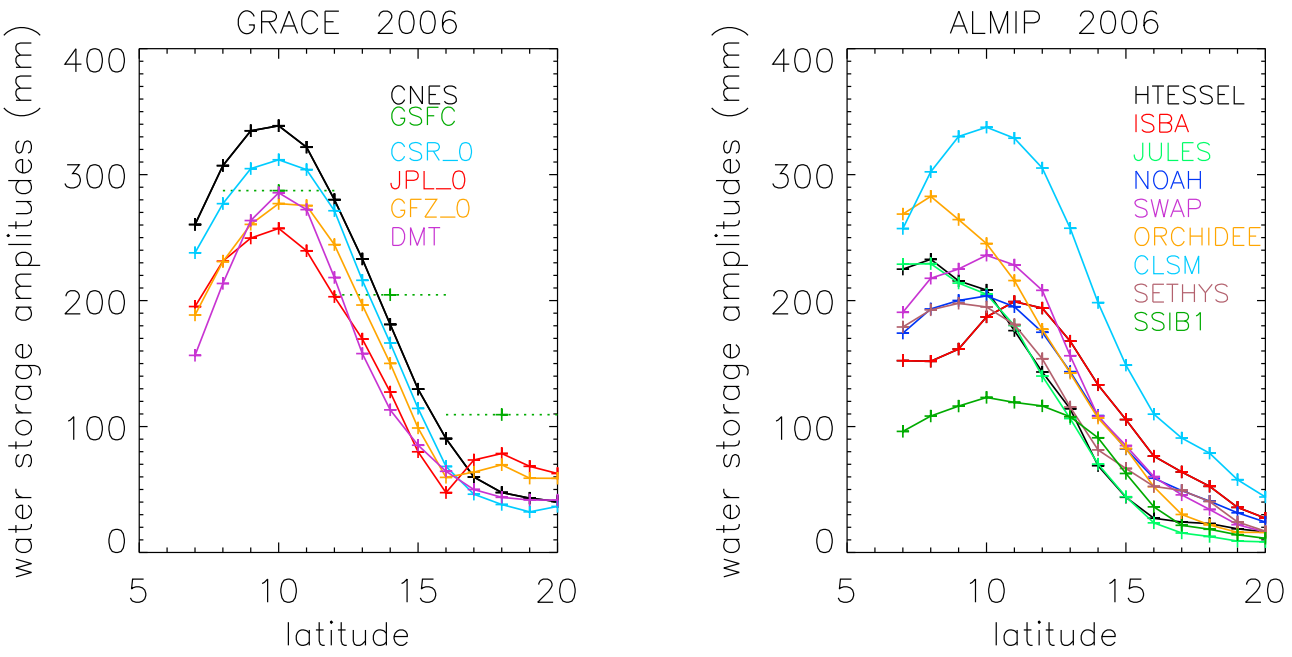

Figure 13. Latitudinal distribution (transects of 1° in latitude) averaged over the full longitude extent of the study area of the annual amplitudes (difference between maximum and minimum values) in 2006 estimated by (left) GRACE and (right) ALMIP models.

In general, a good agreement is found between GRACE and ALMIP seasonal water storage variations for both West Africa and the Sahel. To better compare GRACE estimates and ALMIP output over the Sahel, the water in the Niger River and Niger delta has been removed from the GRACE signal and has also been plotted (Figure 11, right, gray curve): GRACE water storage amplitudes are slightly reduced in September and October, but the shape of the seasonal cycle is not substantially changed, in line with the conclusions by *Kim et al.* [2009] for semiarid areas. Correcting for leakage effects, as discussed in section 2.1.1, may further reduce GRACE amplitudes over the Sahel and make them more consistent with ALMIP amplitudes. Mean total runoff by ALMIP (also shown in Figure 11) is between 0 and 15 mm, so the effects of its redistribution on water storage amplitudes cannot be higher than 15 mm. Also, ALMIP models do not explicitly account for the water table, which could increase the water storage amplitudes. Given that over the Sahel seasonal water storage amplitudes by GRACE and ALMIP are of the same order, groundwater level variations, not represented in land surface models, do not seem to be the most significant factor affecting water stock variations in this region.

[40] Instead, for the West Africa box, GRACE amplitudes may be underestimated because of leakage effects, which could therefore enhance the difference between GRACE and ALMIP. This suggests a more important role of slow reservoirs (rivers, dams, and aquifers) in the southern part of the study region.

[41] Regarding the shape of the seasonal cycle, a steeper slope is observed for GRACE than for ALMIP during the drying-up phase (January–April) for both the West Africa and the Sahel boxes. Only two models (ISBA and CLSM (Figure 12, top)) show a depletion of available moisture comparable to GRACE results in the Sahel. As shown in Figure 12 (middle), this is mainly due to differences in the formulation of dry season evaporation. Indeed, for ISBA and CLSM, evapotranspiration during the dry season over the Sahel is about double than that for the other ALMIP models (for example, average values between January and April are 14 mm/month for ISBA and 12 mm/month for CLSM). In the case of ISBA, the bare soil parametrization includes water vapor transfer in addition to liquid water transfer, allowing a more efficient drying of the surface layer that may therefore enhance evaporation during the dry season. For the CLSM model, the representation of a saturated zone and of subgrid heterogeneity, redistributing water within the pixel in ponds, shallow water table, and temporary flooded areas, results in a longer water retention in the soil layer after the wet season, which allows a sustained evaporation during the dry phases. This longer "memory effect" in the water budget of the CLSM has already been reported by *Mahanama and Koster* [2003].

[42] As far as the wet season is concerned (see also the graphs in Figure 7), soil moisture differences among different models are linked to differences in evapotranspiration for the majority of the models considered here (ISBA, JULES, SWAP, ORCHIDEE, CLSM, and SETHYS) for which slightly higher soil moisture values in the wet season correspond to lower evapotranspiration, which is related to reduced net radiation (not shown). SSIB and NOAH soil moisture anomalies are less related to evapotranspiration: indeed, these two models generate much more total runoff than the land surface model average. In contrast, HTESSEL generates a smaller amount of total runoff than the other models. For HTESSEL and SSIB, these differences can be due to the use of soil and vegetation parameters that are different than the ones employed by the other ALMIP models (which used ECOCLIMAP) (see Table 2). For NOAH, the high total runoff is likely due to the particular scheme

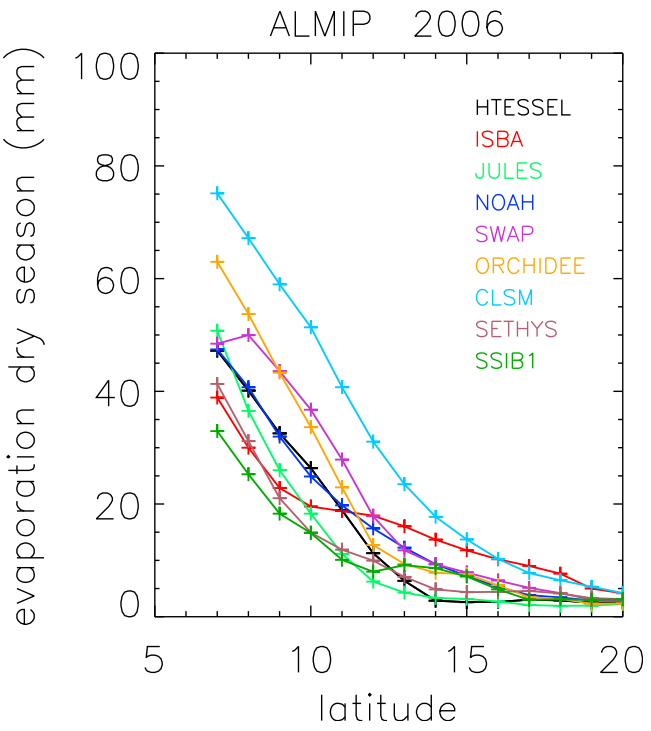

Figure 14. Latitudinal distribution of dry season (December–March) evaporation for the different ALMIP models.

developed by *Decharme* [2007]. Indeed, significant differences in the water budget components are found for models employing the same soil and vegetation parameters. These differences are therefore related to the intrinsic physics of each model and particularly the runoff scheme. CLSM stands apart from the other models and shows a shift in the seasonal evolution of evapotranspiration that is more delayed into the season with a maximum arriving about 1 month after the other models, which is related to the long memory effect discussed above. It should be noted that the inter-model scatter in the ALMIP models is consistent with other similar off-line model intercomparison projects (see a recent example by *Dirmeyer et al.* [2006]).

[43] In terms of the seasonal cycle phase, GRACE wetting and drying-up periods are generally delayed in comparison to ALMIP results. A similar shift of about 1 month has been also reported by *Schmidt et al.* [2008], who compared GRACE and models with estimations over 18 drainage basins in the world, and was attributed to the incomplete description of water lateral transfers in the water storage modeling. The inclusion of a slow reservoir, accounting for processes such as surface runoff routing and drainage into deeper soil layers, could change the shape of the seasonal cycle, with more water being retained after the wet season and being evacuated progressively during the dry season instead of being immediately lost by runoff and drainage. However, *Winsemius et al.* [2006] and *Klokocnik et al.* [2008] also found temporal shifts and hypothesize that these could be caused by leakage or the irregular sampling of the GRACE satellites.

3.3. Zonal Distribution of Land Water Storage

[44] Figure 13 shows the zonal distribution of soil water storage amplitudes, which have been calculated as the difference between the maximum and the minimum values for each latitudinal band for the different GRACE products and the different ALMIP models in 2006. The absolute values of the amplitudes vary among GRACE products, but the shape of their zonal distribution is quite similar for all the products, with a well-defined peak at about 10°N (except for the GFSC solution, for which spatial resolution of 4° × 4° is not fine enough to determine the shape of the zonal curve). A more important spread in the absolute values of the amplitudes is observed for the ALMIP results, with CLSM much higher and SSIB much lower than the average. Moreover, model outputs do not agree on the shape of the latitudinal distribution, with peaks scattered between 8°N and 11°N. These differences seem to be at least partially explained by evapotranspiration differences during the dry season. As shown in Figure 14, models with higher evapotranspiration between December and March correspond to models with higher soil moisture seasonal amplitudes and vice versa. CLSM exhibits again a distinct behavior (Figures 13 and 14), which is consistent with its formulation as it is the only land surface model that includes a water table and the effect of deep soil moisture memory. However, *Gascoin et al.* [2009] showed that this water table may be insufficient to capture large regional aquifer dynamics.

[45] We already discussed the role of evapotranspiration during the dry season to explain the soil moisture seasonal curve over the Sahel (Figure 11, right). The results reported here show that dry season evapotranspiration also plays an important role in the area to the south of the study region (Figures 13 and 14).

3.4. Interannual Variability

[46] Interannual variability has been evaluated by subtracting the mean seasonal cycle (shown in Figure 9) from the water storage temporal evolution in Figure 7. The results are shown in Figure 15 for the Sahel box. For clarity, the wet season (August–November) and the rest of the year (December–July) are reported separately. From August to November, a promising good agreement is found between GRACE and ALMIP: both clearly show, for example, the wet conditions at the end of the 2003 rainy season that was rather good in term of precipitation amount, the important and dramatic drought that affected the Sahel at the end of 2004, the early onset of the monsoon in 2005, and the delayed onset in 2007 and 2006. Similar results (not shown) have been found for the entire West African region. In the December–July period, ALMIP models do not show a significant interannual variability except for a small signature from the previous wet season evident at the end of 2003 and of 2004, which are the extreme wet and dry years. This may be due to the fact that the ALMIP simulations, except for the CLSM model, do not have strong dynamics in the soil layer below the root zone. On the contrary, GRACE estimates indicate large interannual water storage variations for the December–July period as well. This could be due to variability in slow water reservoirs that are not well accounted for by models. Even if noise in the GRACE water height solutions may affect the results, the GRACE interannual signature during the dry season is consistent with precipitation in the previous rainy season. GRACE data therefore provide a base to study memory effects and particularly the

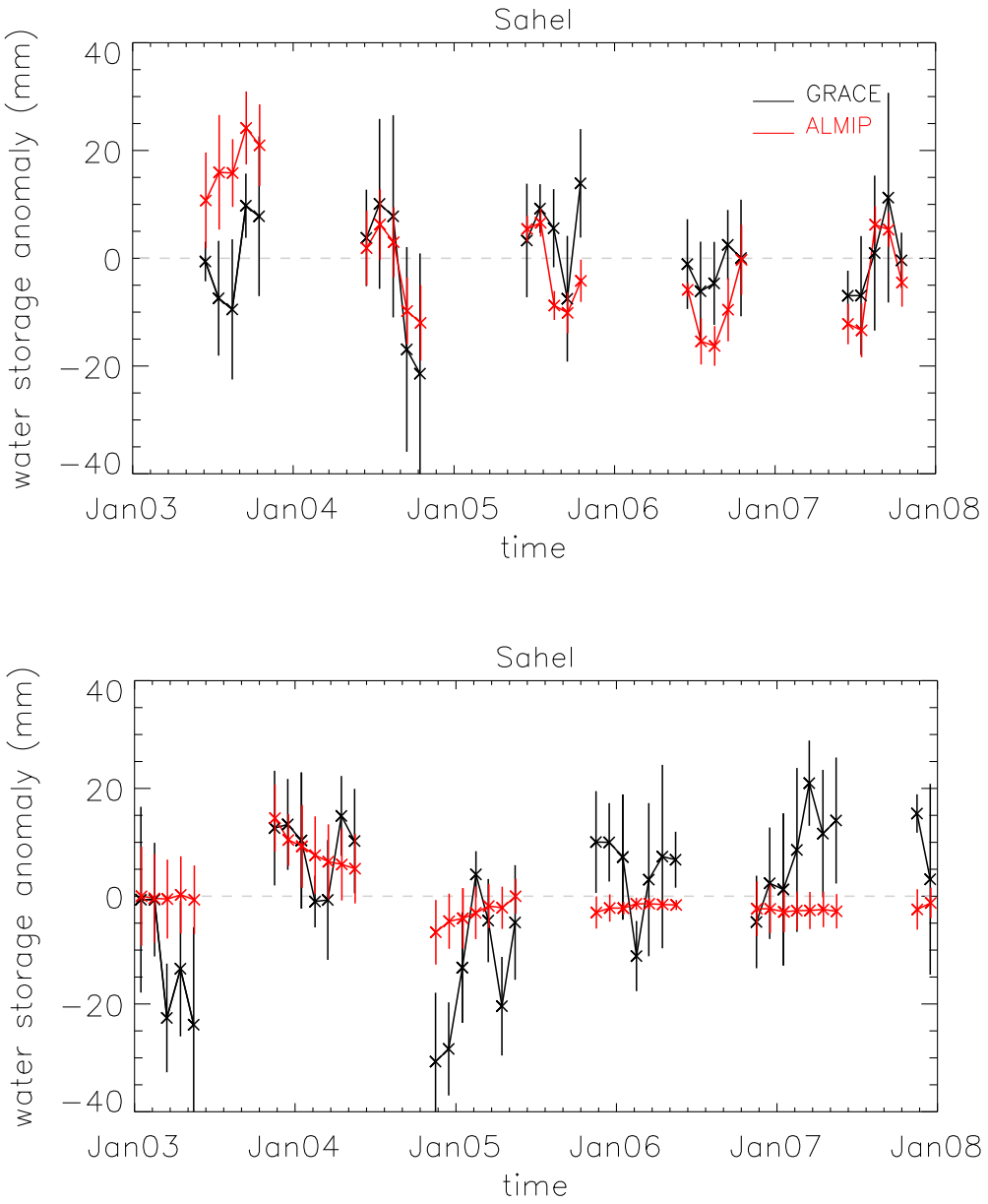

Figure 15. Interannual variations (temporal evolution minus seasonal cycle) in the water storage estimations by GRACE (multisolutions mean and standard deviation) and ALMIP (multimodels mean and standard deviation) during the (top) August–November (top) and (bottom) December–July periods.

Table A1. Characteristics of the Altimetry Stations Used to Estimate Water Mass in the Niger River in the Sahel Box

Station ID	Latitude	Longitude	Minimum Width (m)	Maximum Width (m)	River Length (km)
259	13.18	352.89	600	3090	295.0
173	13.72	354.20	300	2400	87.0
459	16.67	357.11	600	2100	23.5
388	16.73	357.44	1000	4000	43.5
917	16.83	357.80	400	1500	49.0
846	16.92	358.20	380	1500	45.5
373	17.01	358.47	500	4500	60.5
302	17.01	358.94	260	1550	58.0
831	17.00	359.19	400	2000	55.0
760	16.94	359.64	500	7000	102.5
287	15.96	0.15	370	2800	183.0
745	14.31	1.25	550	2900	633.5

Table A2. Monthly Evaporation Rate (mm)[a]

Jan	Feb	Mar	Apr	May	Jun	Jul	Aug	Sep	Oct	Nov	Dec
167	187	212	219	230	215	205	170	173	180	180	160

[a]After *Quensière et al.* [1994].

impact of the previous monsoon season on the following monsoon onset.

4. Concluding Discussion

[47] The results of this study show that GRACE products provide useful detection of water storage changes over West Africa and the Sahel. An important outcome of this study is that GRACE data are able to reproduce the water storage interannual variability over the Sahel. This is encouraging for water storage monitoring and trend detection, which will be possible when satellite gravimetry data is available over a sufficiently long time period.

[48] Substantial uncertainties remain in terms of the magnitudes estimated by the different GRACE products. The effects of leakage on the estimated water storage variations by GRACE could account for a part of the observed discrepancies, but they should not substantially change the results presented here, at least over the Sahel. Indeed, for the large domains used in this study, the differences among different GRACE solutions, accounted for by the multiproduct analysis carried out here, are higher than the estimated effects of leakage.

[49] The comparison between GRACE products and ALMIP soil moisture estimations allowed the identification of the most critical processes that need to be taken into account to improve water storage modeling over the study area. In line with the findings of other studies comparing GRACE products and land surface model outputs over different areas [*Ngo-Duc et al.*, 2007; *Niu et al.*, 2007; *Güntner*, 2008; *Syed et al.*, 2008; *Kim et al.*, 2009; *Alkama et al.*, 2010], the inclusion of slow water reservoirs and transfer schemes routing total runoff in the land surface models could improve the agreement between satellite and model estimates in West Africa. Moreover, we have shown that dry season processes, in particular, evapotranspiration, play an important role in the modeling of soil moisture over the Sahel. This is also the case in the southern part of the study region where vegetation effects are more important. Even when using the same soil and vegetation input data (soil type, soil depth, vegetation type, and root depth), models differ in the soil moisture estimations. The simulation of the dynamics of the deepest soil layers is therefore a critical issue, particularly concerning processes related to vertical transfers upward and downward, horizontal heterogeneity, transpiration through deep roots, and gas phase transfers for dry soil evaporation. This further points out the value of GRACE satellite data for water cycle–related studies in this region where observations are quite scarce and modeling is difficult.

Appendix A

[50] Monthly Niger height levels averaged over 2002–2007 have been derived from altimetry data at twelve locations in the Sahel box (Table A1). For each station, river width at the minimum and maximum river height has been derived from Landsat and Google Earth imagery, and the river cross section for each month's data has been estimated assuming a trapezoidal section. The length of the river corresponding to each location (the characteristics of which are summarized in Table A1) has been derived from Google Earth imagery, excluding the delta (Kirango to Dire). The total length of the Niger River in the Sahel box is 1636 km (delta excluded).

[51] The water budget of the delta can be written as

$$\frac{\Delta D}{\Delta t} = F_{\text{in}} - F_{\text{out}} - \text{ETR}_{\text{delta}} + (R_{\text{local}} + P_{\text{local}} + I),$$

where D is the mass of water, F_{in} is the water entering the delta measured at Kirango and Douna and exiting the delta at Dire (data obtained from GRDC at http://www.grdc.sr.unh.edu/), and $\text{ETR}_{\text{delta}}$ represents evaporation losses in the delta. The other terms are precipitation on the delta, P_{local}, small range runoff contributing to the delta, R_{local}, and exchanges with water tables, I, which are neglected [*Mahé et al.*, 2009]. $\text{ETR}_{\text{delta}}$ is computed as the product of the flood surface S_{delta} by monthly evaporation rate for open water E given by *Quensière et al.* [1994] and in Table A2 as

$$\text{ETR}_{\text{delta}} = E(S_{\text{delta}}).$$

[52] The flooded surface is estimated for 2003 using equations given by *Zwarts and Grigoras* [2005] for expanding and receding periods on the basis of water height data recorded at Akka and Landsat images. To ensure consistency, monthly ETR for 2003 has been rescaled so that annual ETR corresponds to annual $F_{\text{in}} - F_{\text{out}}$, which is measured over 1922–1992.

[53] **Acknowledgments.** First of all, the authors deeply acknowledge all the participants in the ALMIP Working Group (A. Boone, P. de Rosnay, G. Balsamo, A. Beljaars, F. Chopin, B. Decharme, C. Delire, A. Ducharne, S. Gascoin, M. Grippa, F. Guichard, Y. Gusev, P. Harris, L. Jarlan, L. Kergoat, E. Mougin, O. Nasonova, A. Norgaard, T. Orgeval, C. Ottlé, I. Poccard-Leclercq, J. Polcher, I. Sandholt, S. Saux-Picart, and C. Taylor): without their effort on the ALMIP project this study would not have been possible. Many thanks to Anny Cazenave and Ines Fung for useful discussions about GRACE and to Luc Seguis for providing his expertise and feedback on the hydrology of the Soudanian West African region. We also acknowledge Laurent Longuevergne and three anonymous reviewers who carefully read the first version of this manuscript and provided useful comments by which the final manuscript was greatly improved. This work was undertaken under the AMMA project. AMMA, which was based on a French initiative, was built by an international scientific group and is currently funded by a large number of agencies, especially from France, the United Kingdom, the United States, and Africa. It has been the beneficiary of a major financial contribution from the European Community's Sixth Framework Research Programme. F. Frappart was funded by a CNRS postdoctoral grant. GRACE CSR, JPL, and GFZ data were processed by D. P. Chambers and were supported by the NASA Earth Science REASoN GRACE Project. Altimetry data have been provided by J. F. Cretaux.

References

Alkama, R., B. Decharme, H. Douville, M. Becker, A. Cazenave, J. Sheffield, A. Voldoire, S. Tyteca, and P. Le Moigne (2010), Global evaluation of the ISBA-TRIP continental 1 hydrologic system. Part 1: A twofold constraint using GRACE terrestrial water storage estimates and in-situ river discharges, *J. Hydrometeorol.*, *11*, 583–600.

Andersen, O. B., S. I. Seneviratne, J. Hinderer, and P. Viterbo (2005), GRACE-derived terrestrial water storage depletion associated with the 2003 European heat wave, *Geophys. Res. Lett.*, *32*, L18405, doi:10.1029/2005GL023574.

Balsamo, G., P. Viterbo, A. Beljaars, B. van den Hurk, M. Hirsch, A. Betts, and K. Scipal (2009), A revised hydrology for the ECMWF model: Verification from field site to terrestrial water storage and impact in the Integrated Forecast System, *J. Hydrometeorol.*, *10*, 623–643.

Boone, A., et al. (2009), The AMMA Land Surface Model Intercomparison Project (ALMIP), *Bull. Am. Meteorol. Soc.*, *90*(12), 1865–1880.

Braud, I., P. Bessemoulinb, B. Montenyc, M. Sicot, J. P. Vandervaerea, and M. J. Vauclina (1997), Unidimensional modelling of a fallow savannah during the HAPEX-Sahel experiment using the SiSPAT model, *J. Hydrol.*, *188–189*, 912–943.

Bruinsma, S., J.-M. Lemoine, R. Biancale, and N. Valès (2010), CNES/GRGS 10-day gravity field models (release 2) and their evaluation, *Adv. Space Res.*, *45*, 587–601.

Chambers, D. P. (2006), Evaluation of new GRACE time-variable gravity data over the ocean, *Geophys. Res. Lett.*, *33*, L17603, doi:10.1029/2006GL027296.

Chen, F., and J. Dudhia (2001), Coupling an advanced land surface-hydrology model with the Penn State-NCAR MM5 modelling system. Part I: Model implementation and sensitivity, *Mon. Weather Rev.*, *129*, 569–585.

Chen, J. L., C. R. Wilson, J. S. Famiglietti, and M. Rodell (2005), Spatial sensitivity of the Gravity Recovery and Climate Experiment (GRACE) time-variable gravity observations, *J. Geophys. Res.*, *110*, B08408, doi:10.1029/2004JB003536.

Chen, J. L., C. R. Wilson, B. D. Tapley, Z. L. Wang, and G. Y. Niu (2009), 2005 drought event in the Amazon River basin measured by GRACE and estimate by climate models, *J. Geophys. Res.*, *114*, B05404, doi:10.1029/2008JB006056.

Crowley, J. W., J. X. Mitrovica, R. C. Bailey, M. E. Tamisiea, and J. L. Davis (2006), Land water storage within the Congo Basin inferred from GRACE satellite gravity data, *Geophys. Res. Lett.*, *33*, L19402, doi:10.1029/2006GL027070.

Decharme, B. (2007), Influence of the runoff representation on continental hydrology using the NOAH and the ISBA land surface models. *J. Geophys. Res.*, *112*, D19108, doi:10.1029/2007JD008463.

de Rosnay, P., J. Polcher, M. Bruen, and K. Laval (2002), Impact of a physically based soil water flow and soil-plant interaction representation for modeling large-scale land surface processes., *J. Geophys. Res.*, *107*(D11), 4118, doi:10.1029/2001JD000634.

Descroix, L., et al. (2009), Spatio-temporal variability of hydrological regimes around the boundaries between Sahelian and Sudanian areas of West Africa: A synthesis, *J. Hydrol.*, *375*, 90–102.

Dirmeyer, P. A., X. Gao, M. Zhao, Z. Guo, T. Oki, and N. Hanasaki (2006), GSWP-2: Multi-model analysis and implications for our perception of the land surface, *Bull. Am. Meteorol. Soc.*, *87*, 1381–1397.

d'Orgeval, T., J. Polcher, and P. de Rosnay (2008), Sensitivity of the West African hydrological cycle in ORCHIDEE to infiltration processes, *Hydrol. Earth Syst. Sci. Discuss.*, *5*, 2251–2292.

Essery, R. L. H., M. Best, R. Betts, P. Cox, and C. M. Taylor (2003), Explicit representation of subgrid heterogeneity in a GCM land surface scheme, *J Hydrometeorol.*, *4*, 530–543.

Favreau, G., B. Cappelaere, S. Massuel, M. Leblanc, M. Boucher, N. Boulain, and C. Leduc (2009), Land clearing, climate variability, and water resources increase in semiarid southwest Niger: A review, *Water Resour. Res.*, *45*, W00A16, doi:10.1029/2007WR006785.

Frappart, F., G. Ramillien, M. Leblanc, S. O. Tweed, M.-P. Bonnet, and P. Maisongrande (2011), An independent component analysis filtering approach for estimating continental hydrology in the GRACE gravity data, *Remote Sens. Environ.*, *115*, 187–204.

Gascoin, S. (2009), Etude des paramétrisations hydrologiques d'un modèle de surface continentale: Importance des aquifères et des premiers centimètres du sol, Ph.D. thesis, Univ. Pierre et Marie Curie, Paris. [Available at http://tel.archives-ouvertes.fr/.]

Giannini, A., R. Saravanan, and P. Chang (2003), Oceanic forcing of Sahel rainfall on interannual to interdecadal time scales, *Science*, *302*, 1027–1030.

Giannini, A., M. Biasutti, and M. M. Verstraete (2008), A climate model-based review of drought in the Sahel: Desertification, the re-greening and climate change, *Global Planet. Change*, *64*, 119–128.

Güntner, A. (2008), Improvement of global hydrological models using GRACE data, *Surv. Geophys.*, *29*, 375–397.

Gusev, E. M., O. N. Nasonova, and E. E. Kovalev (2006), Modeling the components of heat and water balance for the land surface of the globe, *Water Resour.*, *33*, 616–627.

Huffman, G. J., R. F. Adler, D. T. Bolvin, G. Gu, E. J. Nelkin, K. P. Bowman, Y. Hong, E. F. Stocker, and D. B. Wolff (2007), The TRMM multi-satellite precipitation analysis: Quasi-global, multi-year, combined-sensor precipitation estimates at fine scale, *J. Hydrometeorol.*, *8*, 38–55.

Kim, H., P. J.-F. Yeh, T. Oki, and S. Kanae (2009), Role of rivers in the seasonal variations of terrestrial water storage over global basins, *Geophys. Res. Lett.*, *36*, L17402, doi:10.1029/2009GL039006.

Klees, R., E. A. Zapreeva, H. C. Winsemius, and H. H. G. Savenije (2007), The bias in GRACE estimates of continental water storage variations, *Hydrol. Earth Syst. Sci.*, *11*, 1227–1241.

Klees, R., X. Liu, T. Wittwer, B. C. Günter, E. A. Revtova, R. Tenzer, P. Ditmar, H. C. Winsemius, and H. H. G. Savenije (2008a), A comparison of global and regional GRACE models for land hydrology, *Surv. Geophys.*, *29*, 335–359.

Klees, R., E. A Rervtova, B. Günter, P. Ditmar, E. Oudman, H. C. Winsemius, and H. H. Savanije (2008b), The design of an optimal filter for monthly GRACE gravity field models, *Geophys. J. Int.*, *175*, 417–432.

Koster, R. D., M. J. Suarez, A. Ducharne, P. Kumar, and M. Stieglitz (2000), A catchment-based approach to modeling land surface processes in a GCM: 1. Model structure, *J. Geophys. Res.*, *105*, 24,809–24,822.

Koster, R. D., et al. (2004), Regions of strong coupling between soil moisture and precipitation, *Science*, *305*, 1138–1140.

Klokocnik, J., C. A. Wagner, J. Kostelecký, A. Bezděk, P. Novák, and D. McAdoo (2008), Variations in the accuracy of gravity recovery due to ground track variability: GRACE, CHAMP, and GOCE, *J. Geod.*, *82*, 917–927.

Klosko, S., D. Rowlands, S. Luthcke, F. Lemoine, D. Chinn, and M. Rodell (2009), Evaluation and validation of mascon recovery using GRACE KBRR data with independent mass flux estimates in the Mississippi Basin, *J. Geod.*, *83*, 817–827.

Kusche, J. (2007), Approximate decorrelation and non-isotropic smoothing of time-variable GRACE-type gravity fields, *J. Geod.*, *81*, 733–749.

Lebel, T., J. D. Taupin, and N. d'Amato (1997), Rainfall monitoring during HAPEX-Sahel: 1. General rainfall conditions and climatology, *J. Hydrol.*, *188–189*, 74–96.

Liu, X. (2008), Global gravity field recovery from satellite-to-satellite tracking data with the acceleration approach, *Publ. Geod. 68*, Ned. Geod. Comm., Delft, Netherlands.

Llubes, M., J.-M. Lemoine, and F. Remy (2007), Antarctica seasonal mass variations detected by GRACE, *Earth Planet. Sci. Lett.*, *260*(1–2), 127–136.

Longuevergne, L., B. S. Scanlon, and C. R. Wilson (2010), GRACE hydrological estimated for small basins: Evaluating processing approaches on the High Plains Aquifer, USA, *Water Resour. Res.*, *46*, W11517, doi:10.1029/2009WR008564.

Mahanama, S. P. P., and R. D. Koster (2003), Intercomparison of soil moisture memory in two land surface models, *J. Hydrometeorol.*, *4*, 1134–1146.

Mahè, G., F. Bamba, A. Soumaguel, D. Orange, and J.-C. Olivry (2009), Water losses in the inner delta of the River Niger: Water balance and flooded area, *Hydrol. Processes*, *23*, 3157–3160, doi:10.1002/hyp.7389.

Ngo-Duc, T., K. Laval, G. Ramillien, J. Polcher, and A. Cazenave (2007), Validation of the landwater storage simulated by Organising Carbon and Hydrology in Dynamic Ecosystems (ORCHIDEE) with Gravity Recovery and Climate Experiment (GRACE) data, *Water Resour. Res.*, *43*, W04427, doi:10.1029/2006WR004941.

Niu, G.-Y., Z.-L. Yang, R. E. Dickinson, L. E. Gulden, and H. Su (2007), Development of a simple groundwater model for use in climate models and evaluation with Gravity Recovery and Climate Experiment data, *J. Geophys. Res.*, *112*, D07103, doi:10.1029/2006JD007522.

Noilhan, J., and J.-F. Mahfouf (1996), The ISBA land surface parameterization scheme, *Global Planet. Change*, *13*, 145–159.

Papa, F., A. Guntner, F. Frappart, C. Prigent, and W. B. Rossow (2008), Variations of surface water extent and water storage in large river basins: A comparison of different global data sources, *Geophys. Res. Lett.*, *35*, L11401, doi:10.1029/2008GL033857.

Peugeot, C., M. Esteves, S. Galle, J. L. Rajot, and J. P. Vandervaere (1997), Runoff generation processes: Results and analysis of field data collected at the east central supersite of the HAPEX-Sahel experiment, *J. Hydrol.*, *189*, 179–202.

Philippon, N., and B. Fontaine (2002), The relantionship between the Sahelian and previous 2nd Guinean rainy seasons: A monsoon regulation by soil wetness?, *Ann. Geophys.*, *20*, 575–582.

Quensire, J., J. C. Olivry, Y. Poncet, and J. Wuillot (1994), Environnement deltaique, in *La Peche Dans le Delta Central du Niger: Approche*

Pluridisciplinaire d'un Systeme de Production Halieutique edited by J. Quensiere, pp. 43–77, ORSTOM-Karthala, Paris.

Ramillien, G., F. Frappart, A. Cazenave, and A. Guntner (2005), Time variations of land water storage from an inversion of 2 years of GRACE geoids, *Earth Planet. Sci. Lett.*, *253*(1–2), 283–301.

Ramillien, G., F. Frappart, A. Guntner, T. Ngo-Duc, A. Cazenave, and K. Laval (2006), Time variations of the regional evapotranspiration rate from Gravity Recovery and Climate Experiment (GRACE) satellite gravimetry, *Water Resour. Res.*, *42*, W10403, doi:10.1029/2005WR004331.

Ramillien, G., J. S. Famiglietti, and J. Wahr (2008a), Detection of continental hydrology and glaciology signals from GRACE: A review, *Surv. Geophys.*, *29*, 361–374.

Ramillien, G., S. Bouhours, A. Lombard, A. Cazenave, F. Flechtner, and R. Schmidt (2008b), Land water storage contribution to sea level from GRACE geoid data over 2003–2006, *Global Planet. Change*, *60*, 381–392.

Rodell, M., J. S. Famiglietti, J. Chen, S. I. Seneviratne, P. Viterbo, S. Holl, and C. R. Wilson (2004), Basin scale estimates of evapotranspiration using GRACE and other observations, *Geophys. Res. Lett.*, *31*, L20504, doi:10.1029/2004GL020873.

Rowlands, D. D., S. B. Luthcke, S. M. Klosko, F. G. R. Lemoine, D. S. Chinn, J. J. McCarthy, C. M. Cox, and O. B. Anderson (2005), Resolving mass flux at high spatial and temporal resolution using GRACE intersatellite measurements, *Geophys. Res. Lett.*, *32*, L04310, doi:10.1029/2004GL021908.

Saux-Picart, S., C. Ottlé, A. Perrier, B. Decharme, B. Coudert, M. Zribi, N. Boulain, B. Cappelaere, and D. Ramier (2009), SEtHyS_Savannah: A multiple source land surface model applied to Sahelian landscapes, *Agric. For. Meteorol.*, *149*(9), 1421–1432.

Schmidt, R., et al. (2006), GRACE observations of changes in continental water storage, *Global Planet. Change*, *50*, 112–126.

Schmidt, R., S. Petrovic, A. Guntner, F. Barthelmes, J. Wunsch, and J. Kusche (2008), Periodic components of water storage changes from GRACE and global hydrology models, *J. Geophys. Res.*, *113*, B08419, doi:10.1029/2007JB005363.

Seitz, F., M. Schmidt, and C. K. Shum (2008), Signals of extreme weather conditions in central Europe in GRACE 4-D hydrological mass variations, *Earth Planet. Sci. Lett.*, *268*(1–2), 165–170.

Sultan, B., and S. Janicot (2003), The West African monsoon dynamics. Part II: The 'preonset' and 'onset' of the summer monsoon, *J. Clim.*, *16*(21), 3407–3427.

Swenson, S., and J. Wahr (2006a), Estimating large-scale precipitation minus evapotranspiration from GRACE satellite gravity measurements, *J. Hydrometeorol.*, *7*, 252–270.

Swenson, S., and J. Wahr (2006b), Post-processing removal of correlated errors in GRACE data, *Geophys. Res. Lett.*, *33*, L08402, doi:10.1029/2005GL025285.

Swenson, S., J. S. Famiglietti, J. Basara, and J. Wahr (2008), Estimating profile soil moisture and groundwater variations using GRACE and Oklahoma Mesonet soil moisture data, *Water Resour. Res.*, *44*, W01413, doi:10.1029/2007WR006057.

Syed, T. H., J. S. Famiglietti, J. Chen, M. Rodell, S. I. Seneviratne, P. Viterbo, and C. R. Wilson (2005), Total basin discharge for the Amazon and Mississippi River basins from GRACE and a land-atmosphere water balance, *Geophys. Res. Lett.*, *32*, L24404, doi:10.1029/2005GL024851.

Syed, T. H., J. S. Famiglietti, M. Rodell, J. Chen, and C. R. Wilson (2008), Analysis of terrestrial water storage changes from GRACE and GLDAS, *Water Resour. Res.*, *44*, W02433, doi:10.1029/2006WR005779.

Winsemius, H. C., H. H. G. Savenije, N. C. Van de Giesen, B. J. J. M. Van den Hurk, E. A. Zapreeva, and R. Klees (2006), Assessment of Gravity Recovery and Climate Experiment (GRACE) temporal signature over the upper Zambezi, *Water Resour. Res.*, *42*, W12201, doi:10.1029/2006WR005192.

Xue, Y., P. J. Sellers, J. L. Kinter, and J. Shukla (1991), A simplified biosphere model for global climate studies, *J. Climate*, *4*, 345–364.

Yirdaw, S. Z., K. R. Snelgrove, and C. O. Agboma (2008), GRACE satellite observations of terrestrial moisture changes for drought characterization in the Canadian Prairie, *J. Hydrol.*, *356*, 84–92.

Zwarts, L., and I. Grigoras (2005), Flooding of the inner Niger delta, in *The Niger, a Lifeline: Effective Water Management in the Upper Niger Basin*, edited by L. Zwarts et al., pp. 43–77, RIZA, Amsterdam.

Q. Araud, F. Frappart, M. Grippa, L. Kergoat, and G. Ramillien, Géosciences Environnement Toulouse, UMR 5563, CNRS-Université Toulouse III-IRD, 14 av. E. Belin, F-31400 Toulouse, France. (araud.quentin@gmail.com; frappart@get.obs-mip.fr; manuela.grippa@get.obs-mip.fr; laurent.kergoat@get.obs-mip.fr; guillaume.ramillien@get.obs-mip.fr)

G. Balsamo and P. de Rosnay, European Centre for Medium-Range Weather Forecasts, Shinfield Park, Reading RG2 9AX, UK. (gianpaolo.balsamo@ecmwf.int; patricia.rosnay@ecmwf.int)

A. Boone and B. Decharme, Centre National de Recherches Météorologiques, 42, av. G. Coriolis, F-31057 Toulouse, France. (aaron.boone@meteo.fr; bertrand.decharme@cnrm.meteo.fr)

S. Gascoin, Centro de Estudios Avanzados en Zonas Aridas, Calle Benavente 980, La Serena, Chile. (simon.gascoin@ceaza.cl)

J.-M. Lemoine, Dynamique Terrestre et Planétaire, UMR 5562, CNRS-UPS Toulouse III, 14 av. E. Belin F-31400 Toulouse, France. (jean-michel.lemoine@cnes.fr)

C. Ottlé, Laboratoire des Sciences du Climat et de l'Environnement, LSCE/IPSL/CEA-CNRS-UVSQ, Centre d'Etudes de Saclay, Orme des Merisiers, F-91191 Gif-sur-Yvette, France. (catherine.ottle@lsce.ipsl.fr)

S. Saux-Picart, Plymouth Marine Laboratory, Prospect Place, The Hoe, Plymouth PL1 3DH, UK. (stux@pml.ac.uk)